Desalination and Water Treatment
www.deswater.com
doi: 10.1080/19443994.2013.794106

52 (2014) 2419–2432
March

Taylor & Francis
Taylor & Francis Group

Modeling and particular application of ASM2d model for describing organic matter and nutrient removal in a novel anaerobic-anoxic/oxic eight-phased system

Saad Abualhail[a,b,c], R. Naseer Mohammed[a,b,c], Lu Xiwu[a,c,*], Zhong Zhaoping[a]

[a]*School of Energy and Environment, Southeast University, Sipailou Road, Nanjing 210096, P.R. China*
Tel. +86 13260780581; email: saadaboalheel@yahoo.com
[b]*Faculty of Engineering, University of Basrah, Basra, Iraq*
[c]*Engineering Research Center of Taihu Lake Water Environment, Southeast University, Linghu Avenue Road, Wuxi 214135, China*

Received 28 July 2012; Accepted 24 March 2013

ABSTRACT

An eight-phased AA/O process has advantages of saving energy power, cost, and enhancing nitrogen and phosphorus removal; it does not need equipment for sludge and mixed liquor recycle and also it required small land for construction. A computer program was built based on activated sludge model No. 2d (ASM2d) for simulating the performance of multi-tank AA/O activated sludge process in Wuxi campus, southeast university. The difficulty of simulation is the system operation with unsteadily state condition. The results indicated that the growth rate constant of ammonia oxidizing bacteria was 1.4 day^{-1} and yield coefficient was 0.14. According to simulation, heterotrophic organism $X_{H,}$ phosphate accumulating organism X_{PAO}, and ammonia oxidizing bacteria X_{AOB} decreased in the anaerobic tanks because of the lysis reaction. Then the $X_{H,}$ X_{PAO}, and X_A increased in the aerobic tanks due to aerobic growth. The heterotrophic microorganism; phosphorus accumulating organism; and autotrophic bacteria concentrations increased in quantities by about 56, 36, and 74% in tank one due to changes in the environmental state condition from anaerobic to aerobic and decreased in quantities by about 20, 44, and 0.14% in the tank three due to changes in the environmental state condition from aerobic to anoxic. The ratio of total nitrifying species to total active biomass varied between 1 and 12% in multi-tank AA/O process. The multi-tank AA/O system achieved 89 ± 1.3%, 87.7 ± 1.1%, 73.6 ± 2.1%, and 83.7 ± 0.9% of chemical oxygen demand, NH_4^+ -N, TN, and total phosphorus (TP) removal efficiencies, respectively, during a six-month operation with the effluent meeting Chinese sewage discharge standard GB18918-Grade A.

Keywords: Wastewater; Multi-tank; AA/O; ASM2d; Modeling; Biomass

1. Introduction

Over the last 10 years, a number of biological nitrogen and phosphorus removal processes have been used to remove phosphorus with simultaneous nitrification and denitrification process. Most of the developed biological nitrogen and phosphorus removal processes consist of a sequential anaerobic and aerobic stage for biological phosphorus removal

*Corresponding author.

and recycle mixed liquor into anoxic zones to prop up the removal efficiency of total nitrogen. This approach required more energy for mixed liquid recirculation or addition of additional carbon substrate for denitrification process in anoxic zones accordingly, increasing the operational cost of these processes. Phosphorus and nitrogen removal enhanced via reconfiguring biological nutrient removal processes through canceling internal mixed liquor recirculation. This was done by configuring the process into anaerobic, oxic, anoxic, oxic zones in sequence in southeast university of China. A flow was fed into the anaerobic/anoxic zone by changing intake location. Many types of micro-organisms involved in the complex biological transformation processes, such as heterotrophic organisms, phosphate accumulating organisms, and autotrophic organisms. In order to understand bacterial reactions in biological nutrient removal processes, many different types of mathematical models have been proposed [1,2] and applied in the biological nutrient removal processes [3–6]. Some of them two-stage nitrification models [7,8] and other multi-stage denitrification models [9,10] were proposed in the biological nutrient removal processes. Although these models could predict nitrification or denitrification successfully, the application of these models were merely related to nitrogen removal, that is, the behaviors of heterotrophic organisms, phosphate accumulating organisms, and autotrophic organisms in both nitrogen and phosphorus removal process were not taken into account simultaneously. Activated sludge model No. 2d represents a model for biological phosphorus removal with simultaneous nitrification–denitrification in activated sludge systems. ASM2d is the extension of ASM2 model where it expanded to include the denitrifying activity of the phosphorus accumulating organism (X_{PAOs}). Since ASM2d model can be described as multi-stage denitrification and phosphorus removal simultaneously, the objectives of this study are listed as follows: (1) to establish a model (Activated Sludge model No. 2d) in which multi-stage denitrification and phosphorus removal were taken into account simultaneously, (2) to validate the model by exploring the consistency between simulated and observed values of different components including soluble COD S_S; NH_4-N; NO_3-N; and PO_4-P in multi-tank AA/O process, and (3) to analyze the kinetics of different microorganisms including heterotrophic organisms, phosphate accumulating organisms, and autotrophic organisms in the multi-tank AA/O process.

2. Materials and methods

2.1. Experimental equipment

The main parts of a pilot plant utilized in this study are the main body which are rectangular box $750 \times 630 \times 900$ mm, air compressor, pre-static pumps, mechanical agitation mixers, PLC programmable logic control, LCD display screen, inlet wastewater electromagnetic valves, outlet water electromagnetic valves, aeration electromagnetic valves, sludge discharge electromagnetic valves PVC pipes, and others. The principle diagram of pilot plant is shown in Fig. 1. The effective water depth in the five-step continuous flow activated sludge system is 650 mm while the total depth is 900 mm. The plane dimensions of tank two, tank three, and tank four are square planes while tank one and tank five are rectangular planes whereas the effective volumes of tank two, tank three, and tank four are $250 \times 250 \times 650$ mm, while for tank one and tank five are $380 \times 290 \times 650$ mm which make volume ratio between rectangular and square tanks, $v_{tank\ one}$/$v_{tank\ two}$, equal 1.75. An operation cycle is composed of two half cycles with same running schemes, in which the raw wastewater flows from tank one to tank five during the first half cycle, and from tank five to tank one during the second; the first half cycle is similar to second half cycle. The scheme of first half cycle is included in Fig. 1 as bar diagram; it is divided into four phases named as phase I, II, III, and IV, respectively. In this scheme, tank one, tank two, tank three, and tank four operated as reactors and tank five as settler. The direction of flow was changed automatically via changing of intake location so that the system achieved automatic recirculation without equipment to return sludge and mixed liquor. Therefore, this system is effective for reducing energy consumption. Time and environmental state condition were controlled during each phase to achieve the function of AA/O process in the multi-tank system. An optimized removal efficiency of pollutant was achieved at a HRT of 16 h, SRT of 21 day, and air/water ratio of 35% at a temperature range of 19–23°C. The optimized running time was 1.5, 1, 1, and 0.5 h for phase I, II, III, and IV, respectively.

2.2. Data collection and model algorithms

This study was conducted in Wuxi campus, southeast university in four different runs for calibration and parameter estimation and also four different runs for simulation. The raw wastewater was collected from a main manhole every day in a storage tank so it is steady-state simulation. The equations for implementing the calculation of ASM2d were described as

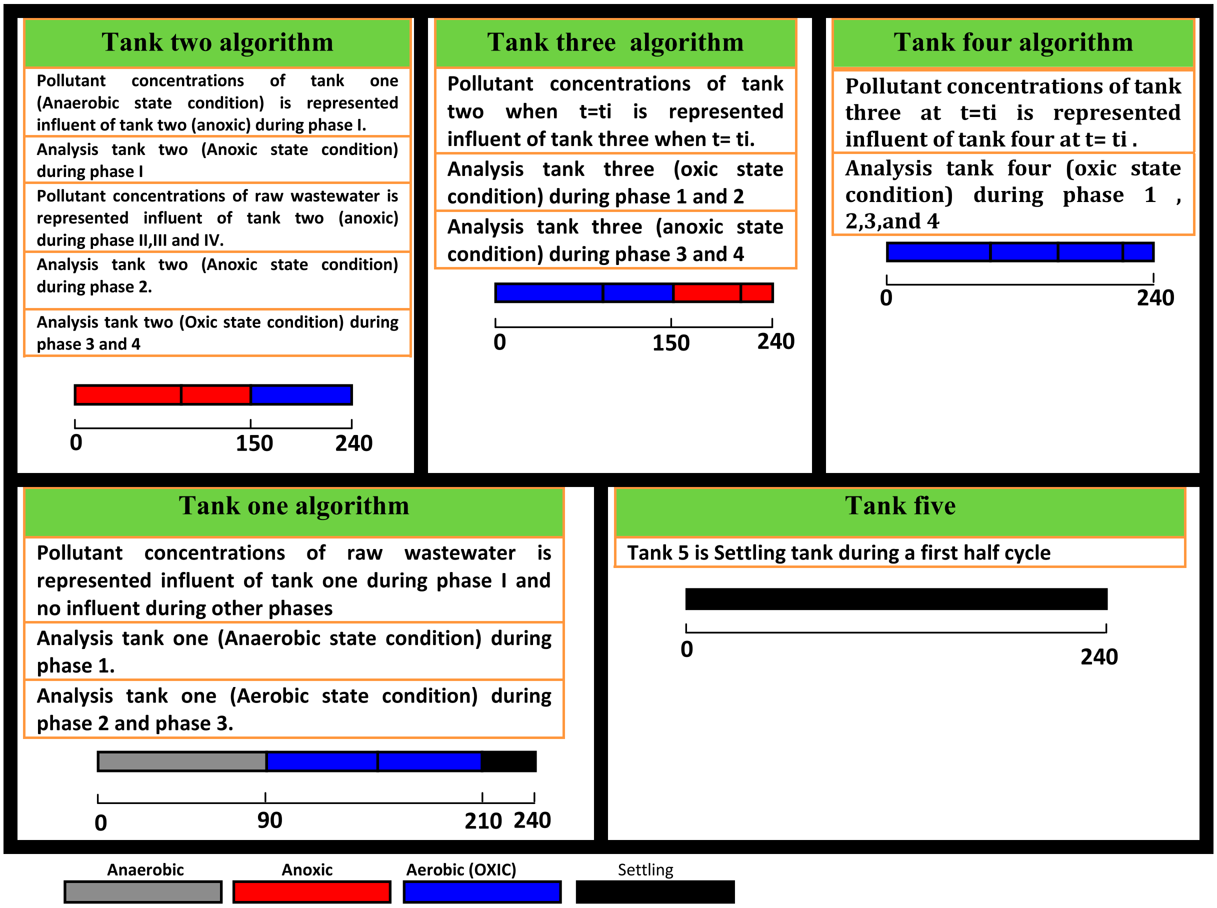

Fig. 1. Layout and algorithms of multi-tank AA/O process during a first half cycle.

follows. First, the basic equation for a mass balance within any defined system boundary was:

$$\text{Input} - \text{Output } t + \text{Reaction} = \text{Accumulation} \quad (1)$$

Therefore, the summary of the mathematical model equations for the reaction rate of each component could be described as in the following equation:

$$C(t) \times (\mathrm{d}C/\mathrm{d}t) = (I_{\mathrm{Ki}} - O_{\mathrm{Ki}} + D_{\mathrm{Ki}} - D_{\mathrm{Ki}})/(V_{\mathrm{Ki}}C_{\mathrm{Ki}}) \quad (2)$$

where I_{ki} and O_{ki} are input (influent) and output transport terms of the ith component in the kth tank; P_{ki} and D_{ki} are production and degradation terms of the ith component in the kth tank; V_{ki} is the volume of the kth tank. The reaction term for the ith component; and r_{i} is obtained by summing the product of the stoichiometric coefficients m_{ij} (Table 1) and the process rate expression e_j (Table 2) for the component i being considered in the mass balance:

$$r_i = \sum_j v_{ij}\rho_j \quad (3)$$

2.3. Sensitivity analysis

The effects of usually large uncertainties parameters in the multi-tank AA/O should be taken into account before starting the simulation of the system via sensitivity analysis. Interval analysis or stochastic techniques could be applied in steady- and transient-state condition [11,12]. In this study, the sensitivity of effluent components for some important parameters was analyzed based on a 5% increased rate in the standard values. All stoichiometrics are four parameters and kinetic parameters include forty-two parameters of ASM2d model. The component concentrations in the influent are sixteen parameters.

The sensitivity analyses of the above parameters (p) with respect to effluent components (E) were calculated by the following equation;

$$\text{Sensitivity} = \frac{\mathrm{d}E/E}{\mathrm{d}p/p} \quad (4)$$

Table 1
Stoichiometric matrix

No.	Process	S_F	S_A	S_{NH}	S_{NO}	S_{PO}	S_I	S_{ALK}	X_S	X_H	X_{PAO}	X_A	X_{PP}	X_{PHA}	X_I	X_{TSS}
1	Aerobic growth on S_F	$-\frac{1}{Y_H}$		$V_{1,NH4}$		$V_{1,PO4}$				1						
2	Aerobic growth on S_A		$-\frac{1}{Y_H}$	$V_{2,NH4}$		$V_{2,PO4}$				1						
3	Anoxic growth on S_F, denitrification (S_{NO})	$-\frac{1}{Y_H}$		$V_{3,NH4}$	$\frac{1-Y_H}{2.85Y_H}$	$V_{3,PO4}$				1						
4	Anoxic growthon S_A, denitrification (S_{NO})		$-\frac{1}{Y_H}$	$V_{4,NH4}$	$\frac{1-Y_H}{2.85Y_H}$	$V_{4,PO4}$				1						
5	Fermentation	−1		$V_{5,NH4}$		$V_{5,PO4}$										
6	Lysis			$V_{6,NH4}$		$V_{6,PO4}$			1-f_{XI}	−1					f_{XI}	
7	Aerobic growth of X_A	$-\frac{3.43-Y_{AOB}}{Y_{AOB}}-\frac{1.14-Y_{NOB}}{Y_{NOB}}$		$V_{7,NH4}$		$-i_{PBM}$						1				
8	Lysis			$V_{8,NH4}$		$V_{8,PO4}$			1-f_{XI}			−1			f_{XI}	
9	Aerobic hydrolysis	1-f_{SI}		$V_{9,NH4}$			f_{SI}	$V_{9,Alk}$	−1							$V_{9,Tss}$
10	Anoxic hydrolysis	1-f_{SI}		$V_{10,NH4}$			f_{SI}	$V_{10,Alk}$	−1							$V_{10,Tss}$
11	Anaerobic hydrolysis	1-f_{SI}		$V_{11,NH4}$			f_{SI}	$V_{11,Alk}$	−1							$V_{11,Tss}$
12	Storage of X_{PHA}		−1			Y_{PO4}							$-Y_{PO4}$	1		
13	Aerobic storage of X_{PP}					−1							1	$-Y_{PHA}$		
14	Anoxic storage of X_{PP}, denitrification (S_{NO})				$V_{15,NO3}$	−1							1	$-Y_{PHA}$		
15	Aerobic growth of X_{PAO}			$V_{16,NH4}$		$-i_{PBM}$					1			$-\frac{1}{Y_H}$		
16	Anoxic growthof X_{PAO}, denitrification (S_{NO})			$V_{17,NH4}$	$-V_{17,NO3}$	$-i_{PBM}$					1			$-\frac{1}{Y_H}$		
17	Lysis of X_{PAO}			$V_{18,NH4}$		$V_{18,PO4}$			1-f_{XI}		−1				f_{XI}	
18	Lysis of X_{PP}					1							−1			
19	Lysis of X_{PHA}		1											−1		

Table 2
Process rate equations

j	Process	Process rate equation $\rho_{j'} \rho_j \geq 0$ ($M_1L^{-3}T^{-1}$)
Heterotrophic organisms: X_H		
1	Aerobic growth on S_F	$\mu_H \frac{S_{02}}{K_{O2H}+S_{O2}} \frac{S_F}{K_{FH}+S_F} \frac{S_F}{S_S+S_F} \frac{S_{NH}}{K_{NH4H}+S_{NH}} \frac{S_{PO}}{K_{PH}+S_{PO}} \frac{S_{ALK}}{K_{ALK+S_{ALK}}} X_H$
2	Aerobic growth on S_A	$\mu_H \frac{S_{02}}{K_{O2H}+S_{O2}} \frac{S_A}{K_{AH}+S_A} \frac{S_A}{S_A+S_F} \frac{S_{NH}}{K_{NH4H}+S_{NH}} \frac{S_{PO}}{K_{PH}+S_{PO}} \frac{S_{ALK}}{K_{ALK+S_{ALK}}} X_H$
3	Anoxic growth on S_F, denitrification (S_{NO})	$\mu_H \eta_{NO3H} \frac{K_{O2H}}{K_{O2H}+S_{O2}} \frac{S_{NO}}{K_{NO3H}+S_{NO}} \frac{S_F}{K_{FH}+S_H} \frac{S_A}{S_A+S_F} \frac{S_{NH}}{K_{NH4H}+S_{NH}} \frac{S_{PO}}{K_{PH}+S_{PO}} \frac{S_{ALK}}{K_{ALK}+S_{ALL}} X_H$
4	Anoxic growth on S_A, denitrification (S_{NO})	$\mu_H \eta_{NO3H} \frac{K_{O2H}}{K_{O2H}+S_{O2}} \frac{S_{NO}}{K_{NO3H}+S_{NO}} \frac{S_A}{K_{FH}+S_F} \frac{S_A}{S_A+S_F} \frac{S_{NH}}{K_{NH4H}+S_{NH}} \frac{S_{PO}}{K_{PH}+S_{PO}} \frac{S_{ALK}}{K_{ALK}+S_{ALL}} X_H$
5	Fermentation	$q_{fe} \frac{K_{O2H}}{K_{O2H}+S_{O2}} \frac{K_{NO3H}}{K_{NO3H}+S_{NO}} \frac{S_F}{K_{fe}+S_F} \frac{S_{ALK}}{K_{ALK}+S_{ALK}} X_H$
6	Lysis	$b_H X_H$
Ammonia oxidizers (nitrifying organisms, autotrophic): X_A		
7	Aerobic growth of X_{AOB}	$\mu_{AOB} \frac{S_{O2}}{K_{O2AOB}+S_{O2}} \frac{S_{NH}}{K_{NH4AOB}+S_{PO}} \frac{S_{ALK}}{K_{ALK}+S_{ALK}} X_{AOB}$
8	Lysis	$b_{AOB} X_{AOB}$
Hydrolysis process		
9	Aerobic hydrolysis	$K_k \frac{S_{O2}}{K_{O2S}+S_{O2}} \frac{X_S/X_H}{K_{XS}+X_S/X_H} X_H$
10	Anoxic hydrolysis	$K_h \eta_{NO3S} \frac{K_{O2S}}{K_{O3S}+S_{O2}} \frac{S_{NO}}{K_{NO3S}+S_{NO}} \frac{X_S/X_H}{K_{XS}+X_S/X_H} X_H$
11	Anaerobic hydrolysis	$K_h \eta_{fe} \frac{K_{NO2S}}{K_{O2S}+S_{O2}} \frac{K_{NO3S}}{K_{NO3S}+S_{NO}} \frac{X_S/X_H}{K_{XS}+X_S/X_H} X_H$
Phosphorus accumulating organisms (PAO): X_{PAO}		
12	Storage of X_{PHA}	$q_{PHA} \frac{S_A}{K_{APAO}+S_A} \frac{S_{ALK}}{K_{ALKPAO}+S_{ALK}} \frac{X_{PP}/X_{PAO}}{K_{PP}+X_{PP}/X_{PAO}} X_{PAO}$
13	Aerobic storage of X_{PP}	$q_{PP} \frac{S_{O2}}{K_{O2PAO}+S_{O2}} \frac{S_{PO}}{K_{PS}+S_{PO}} \frac{S_{ALK}}{K_{ALKPAO}+S_{ALK}} \frac{X_{PHA}/X_{PAO}}{K_{PHA}/X_{PAO}} \frac{K_{MAX}-X_{PP}/X_{PAO}}{K_{IPP}+K_{MAX}-X_{PP}/X_{PAO}} X_{PAO}$
14	Anoxic storage of X_{PP}, denitrification (S_{NO})	$q_{PP} \eta_{NO3PAO} \frac{K_{O2PAO}}{S_{O2}} \frac{S_{NO}}{K_{NO3PAO}+S_{NO}} \frac{S_{O2}}{K_{O2PAO}+S_{O2}} \frac{S_{PO}}{K_{PS}+S_{PO}} \frac{S_{ALK}}{K_{ALKPAO}+S_{ALK}} \frac{X_{PHA}/X_{PAO}}{K_{PHA}+X_{PHA}/X_{PAO}} \frac{K_{MAX}-X_{PP}/X_{PAO}}{K_{IPP}+K_{MAX}-X_{PP}/X_{PAO}} X_{PAO}$
15	Aerobic growth of X_{PAO}	$\mu_{PAO} \frac{S_{O2}}{K_{O2PAO}+S_{O2}} \frac{S_{NH}}{K_{NH4PAO}+S_{NH}} \frac{S_{PO}}{K_{PPAO}+S_{PO}} \frac{S_{ALK}}{K_{ALKPAO}+S_{ALK}} \frac{X_{PHA}/X_{PAO}}{K_{PAH}+X_{PHA}/X_{PAO}} X_{PAO}$
16	Anoxic growth of X_{PAO}, denitrification (S_{NO})	$\mu_{PAO} \eta_{NO3PAO} \frac{K_{O2PAO}}{S_{O2}} \frac{S_{NO}}{K_{NO3PAO}+S_{NO}} \frac{S_{NO}}{K_{O2PAO}+S_{O2}} \frac{S_{NH}}{K_{NH4PAO}+S_{NH}} \frac{S_{PO}}{K_{PPAO}+S_{PO}} \frac{S_{ALK}}{K_{ALKPAO}+S_{ALK}} \frac{X_{PHA}/X_{PAO}}{K_{PHA}+X_{PHA}/X_{PAO}} X_{PAO}$
17	Lysis of X_{PAO}	$b_{PAO} X_{PAO}$
18	Lysis of X_{PP}	$b_{PP} X_{PP}$
19	Lysis of X_{PHA}	$b_{PHA} X_{PHA}$

where dp is the change in the parameter value p and dE is the change in the output E.

The effluent component concentrations (E) have different sensitivities towards different parameters (P) according to sensitivity analysis via above equation. This study showed that the effluent ammonia-nitrogen and nitrate-nitrogen had a sensitivity of more than one towards five parameters, influentNH_4-N, μ_A, Y_{PO4}, q_{pp} and Y_{PO4}; the effluent nitrate-nitrogen had sensitivity of more than one towards four parameters, influent flow-rate, μ_A, Y_H, Y_{PO4}. The effluent PO_4-P has more sensitivity towards PO_4-P, q_{PHA}, q_{PP}, μ_{PAO}, Y_H, K_{MAX}, Y_{PO4}.

2.4. Model calibration

There are many parameters in ASM2d model. For those parameters that are known to be approximately constant in domestic wastewater, the default values from previous research studies [3,13] were used as shown in Table 3.

Model calibration procedure is a process of adjusting coefficient values of the model as shown in Fig. 2, therefore the results simulated by the ASM2d model with these coefficients closely agree with the observed data. The model parameters are highly dependent on environmental state conditions. The parameter values are estimated by minimizing the sum of squares of

Table 3
Raw wastewater characteristics of Wuxi campus, Southeast University

Item	Symbol no.	Concentration (mg/L)			
Case study		1	2	3	4
Total chemical oxygen demand	COD in-filtrated	805	688	458	513
Particulate inert organic material	X_I	63	61	55	59
Slowly biodegradable substrate	X_S	340	297	201	222
Readily biodegradable substrate	S_S	306	261.5	174	195
Active heterotrophic biomass	X_H	5	4	4	1
Active autotrophic biomass	X_A	0.1	0.7	0.3	0.0
Volatile fatty acids	S_A	88	73	61	67
Inert soluble organic material	S_I	7	5	4	4
Oxygen	S_O	0	0	0	0
Nitrate nitrogen	S_{NO}	2.23	1.23	1.26	2.8
Ammonia nitrogen	S_{NH}	18	27	32	19.4
Total nitrogen	TN	31.7	39.6	43.2	33.1
PO_4-P	S_{PO}	2.59	3.25	3.41	1.01
Total nitrogen	TP	3.07	3.71	4.32	1.79
Alkalinity	S_{ALK}	4.97	5.01	4.99	5.00
Mixed liquor suspended solid	MLSS	87	73	71	67

the deviations between the observed data and the model predictions data with the objective function given in the following equation [14]:

$$R^2 = \frac{\sum(\text{Sim} - \text{aobs})^2}{\sum(\text{Sim} - \text{aobs})^2 + \sum(\text{Sim} - \text{obs})^2} \quad (5)$$

where R^2 is the coefficient of determination, sim is the model simulated value, obs is the observed value, and aobs is the average observed value.

The standard deviation for parameter determination was required to be lower than 50% to ensure the validity of the values of the parameters obtained. To make the first move of the calibration procedure, an initial guess of the parameters is essential. Such initial values are obtained with the values in the literature as shown in Table 3. To make simpler calibration process, it is preferred to change little constants as possible, due to the limited changeability of some parameters. The choice of the parameters for calibration is mostly based on the result of sensitivity analysis.

2.5. Analytical methods

COD, NH_4-N, NO_3-N, PO_4-P, TP, and TN were analyzed according to standard methods [16]. NO_3-N were analyzed by the IC method (Metrohm 761 compact IC equipped with metrosep asupp 5 column) and TN was analyzed by analytikjena AG multi N/C 3000.

2.5.1. Biomass batch tests

The procedures were fully or partially adopted from Standard Methods [17] or previous studies [18–21]. In order to determine the kinetic parameters of X_{AOB}, we determined oxygen uptake rate of different microbial functional group for calculation [22,23]. Batch experimental tests were performed for four different runs for determining the kinetic parameters of X_{AOB} and X_{NOB}. The oxygen uptake rate measuring system consisted of four airtight, cylindrical chambers, with same height and volume, four magnetic stirrers for stirring, and an aeration stone in each chamber. DO was monitored by four oxygen meters of high stability connected to a data acquisition system. Since this oxygen uptake rate measurer was airtight, the actual respiration rate of the tested biomass at any time during the batch test did not depend on oxygen input. Therefore, the dissolved oxygen concentration represented the actual oxygen uptake rate. A certain amount of activated sludge sample was taken from the pilot plants and added into oxygen uptake rate chambers. Distilled water containing organic carbon source and nutrient including glucose, NH_4SO_4, and KH_2PO_4 were added resulting in total volume of 800 mL in chamber. The measuring system was periodically aerated, then the difference between the measured OUR and baseline oxygen respiration was calculated and compared. The pH value was maintained at seven during batch test. In order to evaluate the kinetic parameters and active biomass of X_H,

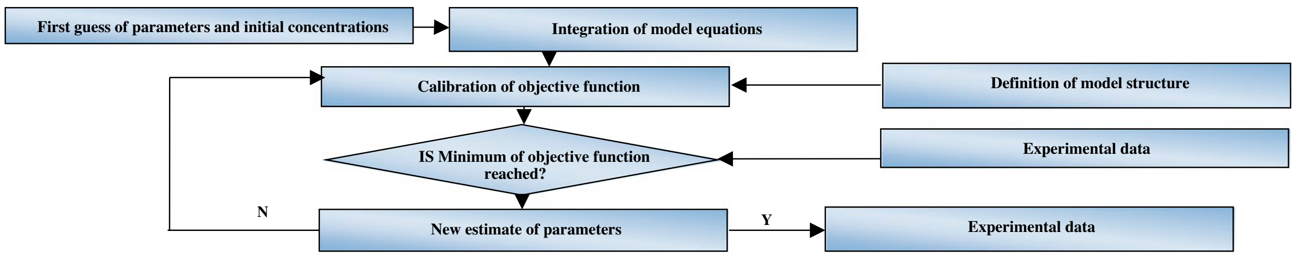

Fig. 2. Illustration of parameter estimation routine [15].

X_{AOB}, and X_{NOB} different types of oxygen uptake rate values should be considered: total oxygen uptake rate (OUR_T), oxygen uptake rate of X_H (OUR_H), and oxygen uptake rate of X_{AOB} (OUR_{AOB}). The determination of oxygen uptake rates of X_H, X_{AOB}, and X_{NOB} was based on the subsequent addition of allylthiourea (ATU) and NaN_3. Allylthiourea (86 µM) was added to the chambers to keep the NH_4-N concentration constant during the incubation by selectively inhibiting X_{AOB} activity without affecting the activity of X_{NOB}, while Azide (86 µM) was added to the chambers to keep the NO_2-N concentration constant during the incubation by selectively inhibiting X_{NOB} activity without affecting the activity of X_{AOB} [24]. When determining OUR_T, no inhibitor was added. When determining OUR_H, both allylthiourea (86 µM) and NaN_3 (24 µM) were added. If only NaN_3 (24 µM) was added, the determined oxygen uptake rate was the sum of OUR_H and OUR_{AOB}, then $OUR_{NOB} = (OUR_H + OUR_{AOB}) - OUR_H$.

2.5.2. PHA test

The initial concentration of PHA in each zone of a new system was analyzed according to the method that is described in Ref. [25] for estimating initial concentration of PHA in each zone. In the initial step, duplicate 20 mL samples of MLSS was obtained and immediately centrifuged at 4˚C. Then, the cold sludge pellet was lyophilized. After that, the pellet was added to the tube closed with a Teflon-lined screw cap for drying. About 2 mL of sulfuric acid, 3% methanol, and 2 mL of chloroform were added to the tube. This was digested for 1,200 min in an oven at 104˚C. At the second step, once the sample had cooled at 25˚C, 1 mL of water was added and the tube contents were shaken for 600 s. The chloroform content remained at the bottom of the tube, and this was drawn off for GC examination. The digested product was exposed on a Varian 3400 GC fitted with a 1.8-m Alltech 0.2% Carbowax 1500 on Graphpac-GC 80/100 mesh stainless steel column. The column temperature was 170˚C and the

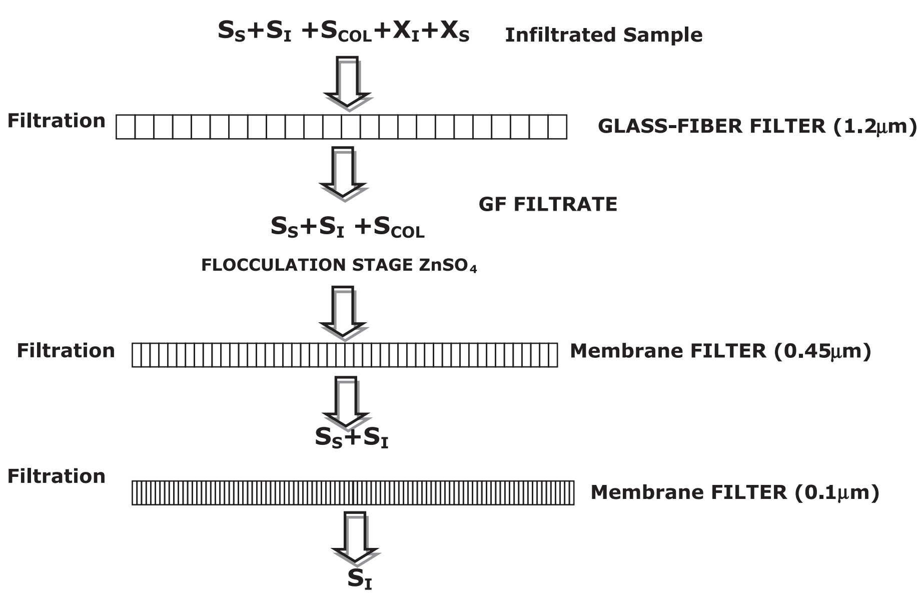

Fig. 3. Diagram depicting the retention/passage of influent wastewater COD components [26].

inoculation temperature was 180˚C. PHA was measured by comparison to a standard consisting of a copolymer of the above-described alkanoates.

2.5.3. Wastewater characterization

Activated sludge models (ASM) distinguish between the mechanisms acting on different components in the influent wastewater stream. The term wastewater characteristic refers to the partitioning of influent organic material into biodegradable and unbiodegradable (inert) portions, the ammonia portion of the total nitrogen, and so on. The influent wastewater is often varied from one municipal wastewater to another. Wastewater characteristics have a very significant impact on system performance, particularly for nutrient removal systems.

Characterization of the carbonaceous material in municipal wastewater for modeling purposes was usually in terms of the chemical oxygen demand (COD). The division of the total influent COD (COD_T) into the various fractions used in nutrient removal system design and modeling is shown in Fig. 3. In ASM2d model, the COD_{tot} of the wastewater consisted of inert soluble organic matter (S_I), readily and slowly biodegradable substrate (S_S and X_S, respectively), and inert suspended organic matter (X_I), whereas biomass in the wastewater is considered to be insignificant.

2.6. Wastewater quality

The raw wastewater used in the experiment was collected from a main manhole of southeast university in Wuxi city and the characteristic of wastewater quality is listed in Table 3. In this study, four testing runs with different operations were implemented in Wuxi campus, southeast university. The raw wastewater is typical in Wuxi city-southeast university, China. COD infiltrated was between 150 and 850 mg/L with average of 650 mg/L, of which S_S, S_I, X_S, and X_I accounted for about 38, 2, 43, and 11%, respectively. MLSS was between 45 and 93 mg/L with average of 76 mg/L. NH_4-N was between 10 and 40 mg/L with average of 22 mg/L. TP was between 1.7 and 4.5 mg/L with average of 2.6 mg/L, of which PO_4-P accounted for about 70–90%.

2.7. Model structure of the system

The model structure was built using stoichiometric matrix Table 1, process rate Table 2, algorithms, and multi-tank AA/O environmental state conditions during each phase. The algorithms of multi-tank AA/O are shown in Fig. 2. The model structure has taken the environmental state condition changing of every tank and phase time into consideration.

The equations that described the transformation of the wastewater quality in the model formed an ordinary differential equations (ODEs) system. The set of equations in this model then was integrated simultaneously by the fourth-order range Kutta numerical analysis integration method [27]. According to the program structure of multi-tank AA/O, the entire model was implemented by means of a computer program that was coded with MATLAB®2010 language. When all the vectors $\frac{1}{C_{ki}}\left(\frac{dC}{dt}\right)$ were nearly equal to zero, a steady state was reached. The integration was most accurate when time step is very small but the computing time increased inversely with the size of time step. Conversely, too large time step would result in large errors and other numerical problems. Thus, one criterion for an upper limit on time step is:

$$\Delta t < -C(t) \times \left(\frac{dC}{ct}\right)^{-1} \tag{6}$$

where Δt is time step. By combining Eqs. (2) and (4), and neglecting the F_{ki} and P_{ki} terms in the mass balance, resulted in an equation for the maximum step size:

$$\Delta t < \frac{V_k C_{ki}}{O_{ki} + K_{ki}} = \theta_{ki} \tag{7}$$

The term θ_{ki} is the mean residence time of component i in reactor component k at steady state.

3. Results and discussion

3.1. Removal efficiency

According to investigation results, this system achieved 89 ± 1.3%, 87.7 ± 1.1%, 73.6 ± 2.1%, and 83.7 ± 0.9% of S_S, NH_4^+-N, TN, and TP removal efficiencies, respectively, during a six-month operation with the effluent meeting Chinese sewage discharge standard GB18918-Grade A. The results showed that this system operates with SND and denitrifying phosphorus removal phenomena which are benefits for enhancing nitrogen and phosphorus removal and also reducing energy power because it needs low dissolved oxygen concentration.

3.2. Model evaluation

The model evaluation is performed from the comparison between the predicated and observed values.

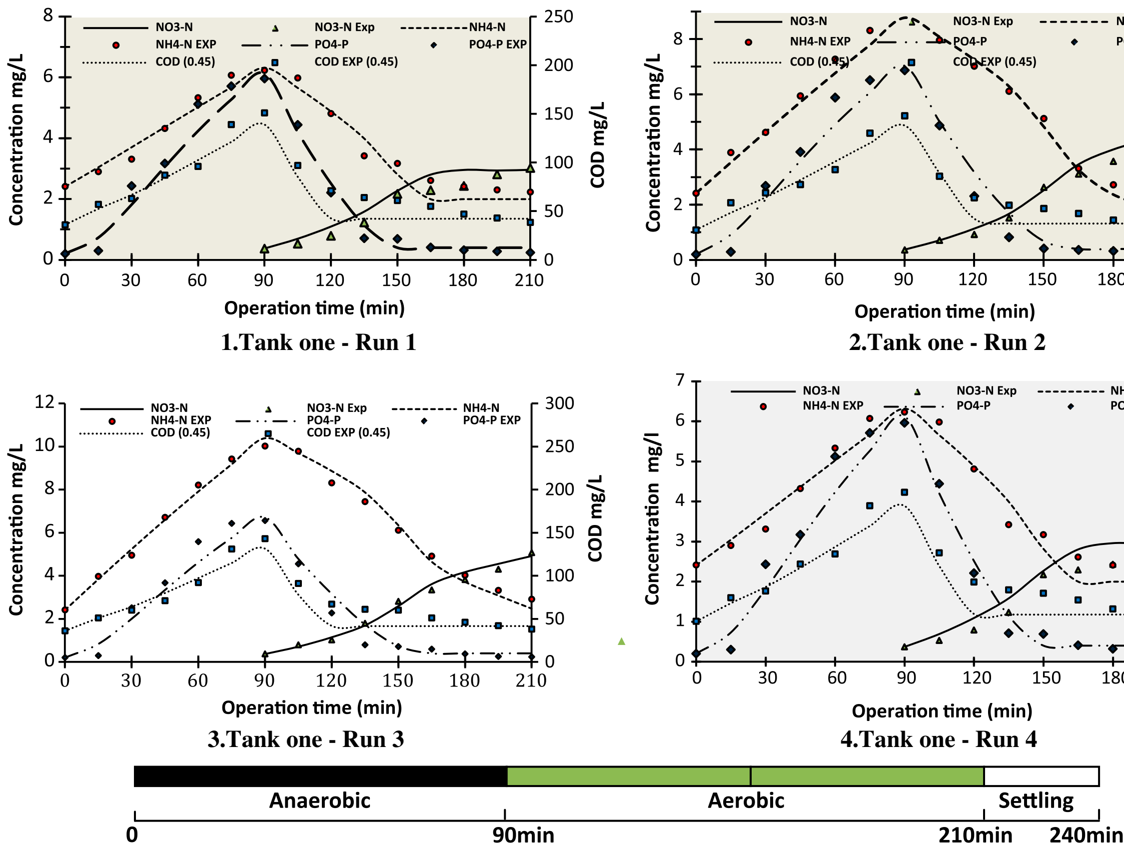

Fig. 4. Simulated and observed COD, NH_4-N, NO_3-N, and PO_4-P in tank one of multi-tank A2/O process.

The experimental data of four related runs in southeast university –Wuxi campus are used for model evaluation. The influent raw wastewater characteristics are shown in Table 3. The predicated and observed are shown in Figs. 4–7 for all related runs. Figs. 4–7 shows the simulated and observed COD, NH_4-N, NO_3-N, and PO_4-P in tank one, tank two, tank three, and tank four, respectively, of multi-tank AA/O activated sludge process. Fig. 4 depicts the observed and predicated data of NH_4-N, PO_4-P, COD, and NO_3-N concentration of tank one under four runs, This figure shows a good consistency between the observed and predicated data whereas the sum of squares of the deviations R^2 of NH_4-N, PO_4-P, COD, and NO_3-N were 0.95, 0.96, 0.93, and 0.98, respectively, at run 1; 0.98, 0.95, 0.91, and 0.97, respectively, at run 2; 0.99, 0.95, 0.87, and 0.99, respectively, at run 3; and 0.95, 0.97, 0.87 and 0.92, respectively, at run 4. Fig. 5 depicts the observed and predicated data of NH_4-N, PO_4-P, COD, and NO_3-N concentration of tank two under four runs. This figure shows a good consistency between the observed and predicated data whereas the sum of squares of the deviations R^2 of NH_4-N, PO_4-P, COD, and NO_3-N were 0.95, 0.73, 0.94, and 0.99, respectively, at run 1; 0.99, 0.89, 0.95, and 0.99, respectively, at run 2; 0.99, 0.89, 0.97, and 0.98, respectively, at run 3; and 0.97, 0.86, 0.97, and 0.98, respectively at run 4. Fig. 6 depicts the observed and predicated data of NH_4-N, PO_4-P, COD, and NO_3-N concentration of tank three under four runs. This figure shows good consistency between the observed and predicated data whereas the sum of squares of the deviations R^2 of NH_4-N, PO_4-P, COD, and NO_3-N were 0.95, 0.66, 0.95, and 0.95, respectively, at run 1; 0.96, 0.77, 0.95, and 0.95, respectively, at run 2; 0.98, 0.63, 0.95, and 0.99, respectively, at run 3; and 0.97, 0.74, 0.95, and 0.997, respectively, at run 4. Fig. 7 depicts the observed and predicated data of NH_4-N, PO_4-P, COD, and NO_3-N concentration of tank four under four runs. This figure shows a good consistency between the observed and predicated data whereas the sum of squares of the deviations R^2 of NH_4-N, PO_4-P, COD, and NO_3-N were 0.96, 0.56, 0.96, and 0.98, respectively, at run 1; 0.97, 0.61, 0.93, and 0.96, respectively, at run 2; 0.99, 0.60, 0.95, and 0.94, respectively, at run 3; and 0.95, 0.59, 0.96, and 0.99, respectively, at run 4.

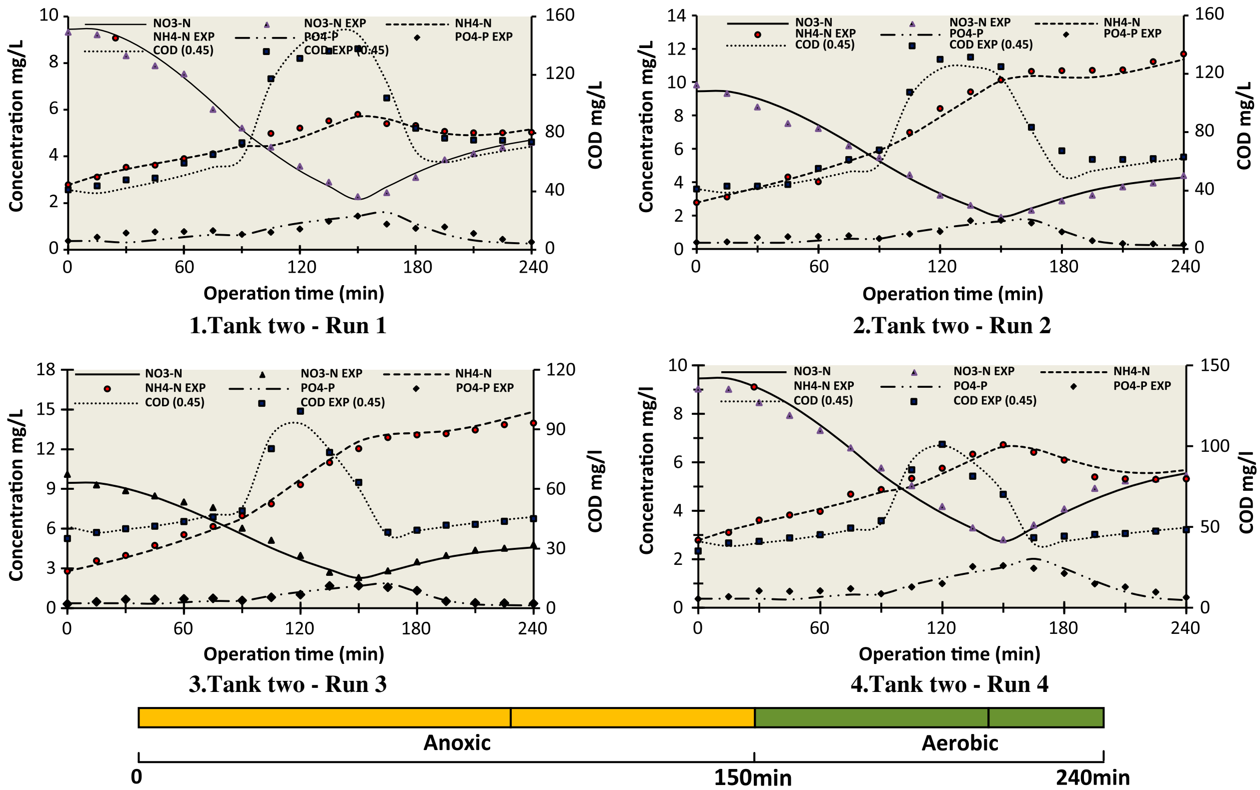

Fig. 5. Simulated and observed COD, NH_4-N, NO_3-N, and PO_4-P in tank two of multi-tank A2/O process.

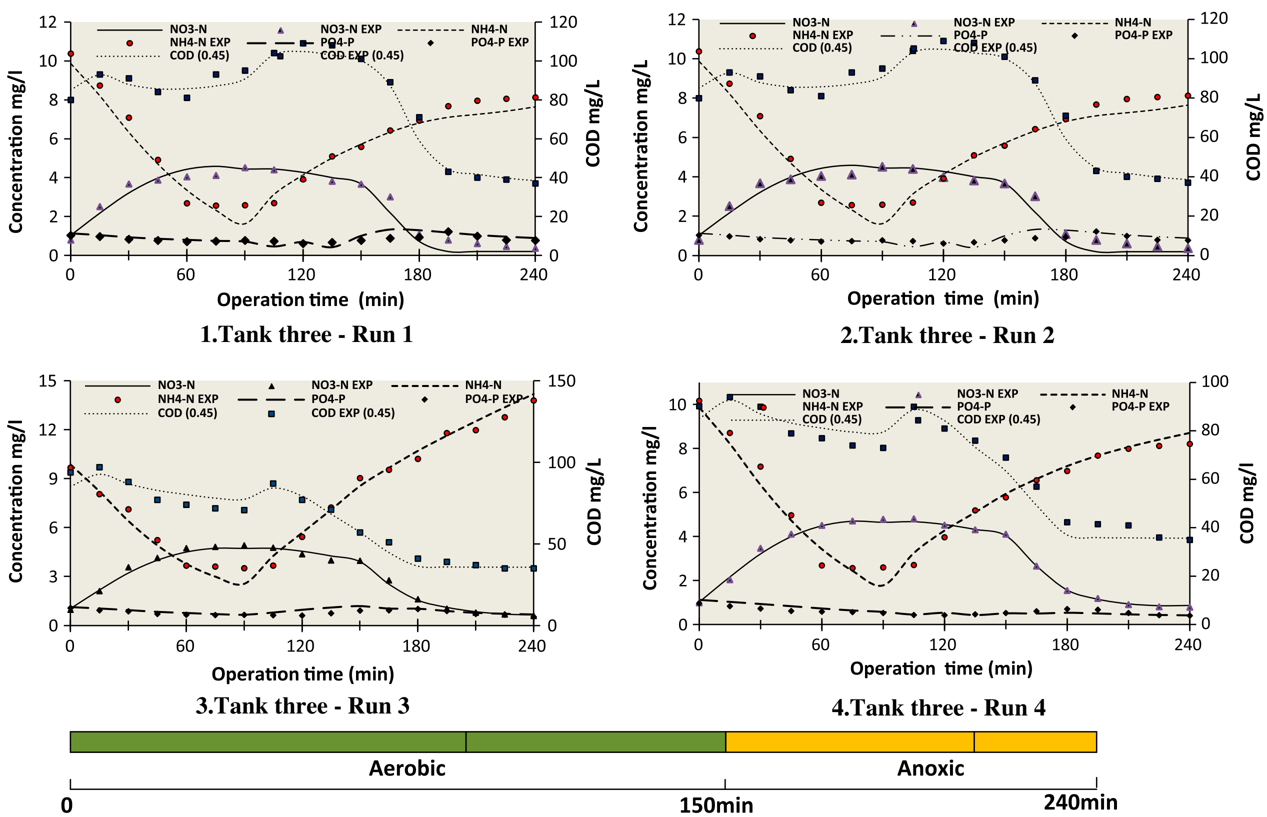

Fig. 6. Simulated and observed COD, NH_4-N, NO_3-N, and PO_4-P in tank three of multi-tank A2/O process.

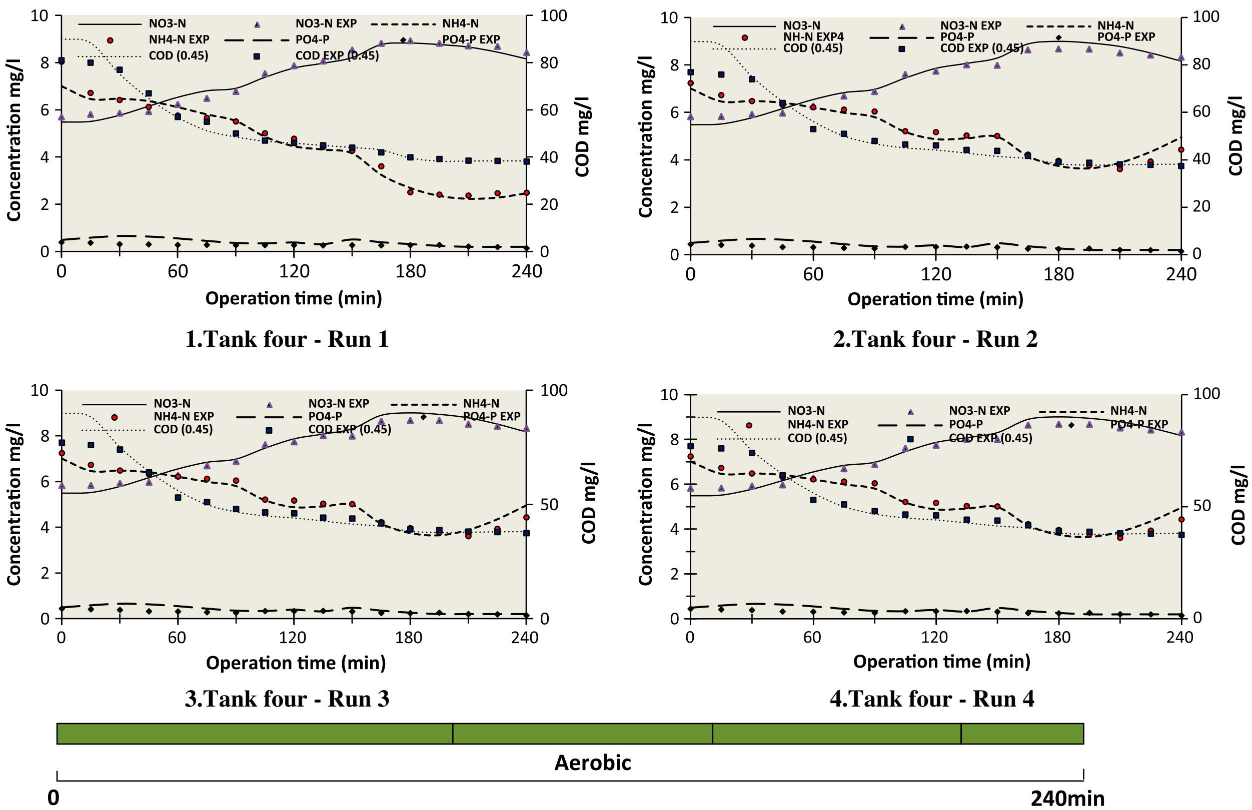

Fig. 7. Simulated and observed COD, NH_4-N, NO_3-N, and PO_4-P in tank four of multi-tank A2/O process.

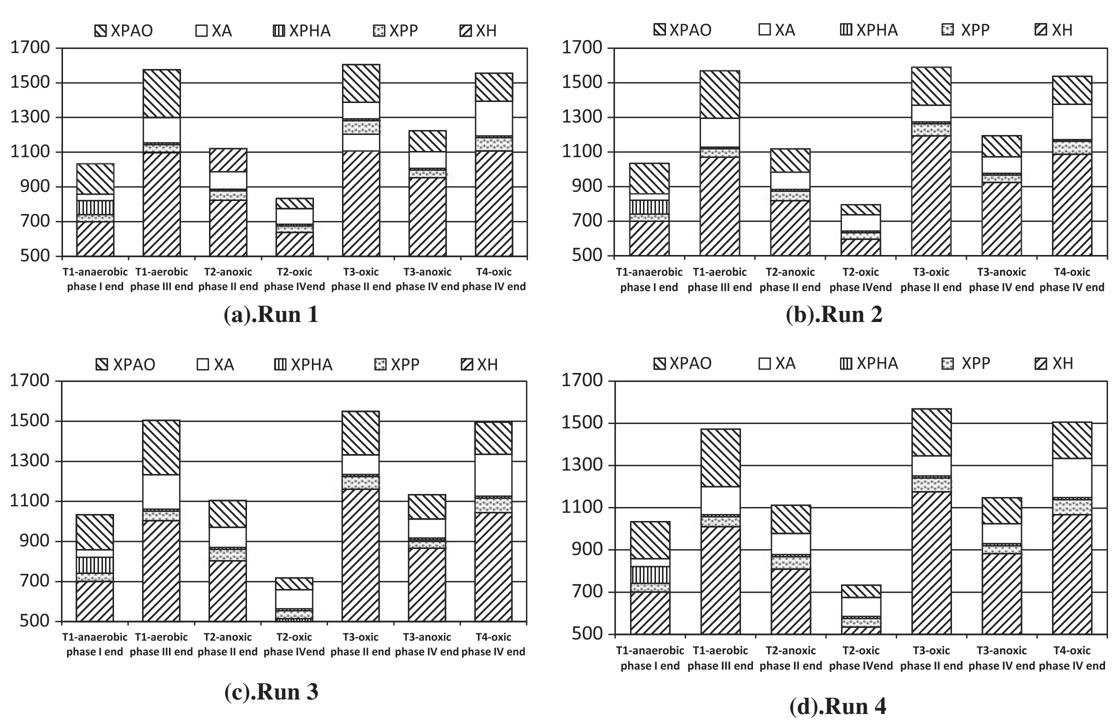

Fig. 8. Variations of biomass in each tank of multi-tank AA/O process.

Table 4
Definition and typical values for kinetic parameters

Item	Description	Ref.	20°c	Units
	Heterotrophic organisms: X_H			
μ_H	Maximum growth rate on substrate	[1]	6.00	g X_S g^{-1} X_H d^{-1}
q_{fe}	Maximum rate for fermentation	Modified	3.3	g X_S g^{-1} X_H d^{-1}
η_{NO3H}	Reduction factor for denitrification (S_{NO})	Modified	0.6	–
b_H	Rate constant for lysis and decay	[1]	0.4	d^{-1}
K_{O2H}	Saturation/inhibition coefficient for oxygen	[1]	0.2	g O2 m^{-3}
K_{FH}	Saturation coefficient for growth on S_F	[1]	4	g COD m^{-3}
K_{fe}	Saturation coefficient for fermentation on S_A	[1]	4	g COD m^{-3}
K_{AH}	Saturation coefficient for growth on acetate S_A	[1]	4	g COD m^{-3}
K_{NO3H}	Saturation/inhibition coefficient for nitrate	[1]	0.5	g N m^{-3}
K_{NH4H}	Saturation coefficient for ammonium (nutrient)	[1]	0.05	g N m^{-3}
K_{PH}	Saturation coefficient for phosphate (nutrient)	[1]	0.01	g N m^{-3}
K_{AL}	Saturation coefficient for alkalinity (HCO_3)	[1]	0.1	mole HCO^{-3} m^{-3}
	Ammonia oxidizers bacteria (nitrifying organisms, autotrophic): X_{AOB}			
μ_{AOB}	Maximum growth rate of X_{AOB}	Modified	1.4	d^{-1}
b_{AOB}	Decay rate of X_{AOB}	Modified	0.08	d^{-1}
K_{O2AOB}	Saturation/inhibition coefficient for oxygen	[1]	0.5	g O2 m^{-3}
K_{NH4AOB}	Saturation coefficient for ammonium (nutrient)	[1]	1	g N m^{-3}
K_{ALKAOB}	Saturation coefficient for alkalinity (HCO^{-3})	[1]	0.5	mole HCO^{-3} m^{-3}
K_{PAOB}	Saturation coefficient for phosphorus (nutrient)	[1]	0.01	g P m^{-3}
	Hydrolysis of particulate substrate: X_S			
K_h	Hydrolysis rate constant	[1]	3	d^{-1}
η_{NO3S}	Anoxic hydrolysis reduction factor	[1]	0.6	–
η_{fe}	Anaerobic hydrolysis reduction factor	[1]	0.4	–
K_{O2S}	Saturation/inhibition coefficient for oxygen	[1]	0.2	g O_2 m^{-3}
K_{NO3S}	Saturation/inhibition coefficient for nitrite and nitrate	[1]	0.5	g N m^{-3}
K_{XS}	Saturation coefficient for particulate COD	[1]	0.1	g X_S g^{-1} X_H
Phosphorus-accumulating organisms: X_{PAO}				
q_{PHA}	Rate constant for storage of X_{PHA} (base X_{PP})	Modified	3.3	g X_{PHA} g^{-1} X_{PAO} d^{-1}
q_{PP}	Rate constant for storage of X_{PP}	[1]	1.5	g X_{PHA} g^{-1} X_{PAO} d^{-1}
μ_{PAO}	Maximum growth rate of PAO	Modified	1.2	d^{-1}
η_{NO3PAO}	Reduction factor for anoxic activity	Modified	0.8	–
b_{PAO}	Rate for lysis of X_{PAO}	[1]	0.2	d^{-1}
b_{PP}	Rate for lysis of X_{PP}	[1]	0.2	d^{-1}
b_{PHA}	Rate for lysis of X_{PHA}	[1]	0.2	d^{-1}
K_{O2PAO}	Saturation/inhibition coefficient for oxygen	[1]	0.2	g O_2 m^{-3}
K_{NO3PAO}	Saturation coefficient for nitrate, S_{NO}	[1]	0.5	g N m^{-3}
K_{APAO}	Saturation coefficient for acetate S_A	[1]	4	g COD m^{-3}
K_{NH4PAO}	Saturation coefficient for ammonium (nutrient)	[1]	0.05	g N m^{-3}
K_{PS}	Saturation coefficient for phosphorus in storage of PP	[1]	0.2	g P m^{-3}
K_{PPAO}	Saturation coefficient for phosphate (nutrient)	[1]	0.01	g P m^{-3}
K_{ALKPAO}	Saturation coefficient for alkalinity (HCO^{-3})	[1]	0.1	mole HCO^{-3} m^{-3}

(*Continued*)

Table 4 (*continued*)

Item	Description	Ref.	20°c	Units
K_{PP}	Saturation coefficient for poly-phosphate	[1]	0.01	$g\ X_{PP}\ g^{-1}\ X_{PAO}$
K_{MAX}	Maximum ratio of X_{PP}/X_{PAO}	[1]	0.34	$g\ X_{PP}\ g^{-1}\ X_{PAO}$
K_{IPP}	Inhibition coefficient for PP storage	[1]	0.02	$g\ X_{PP}\ g^{-1}\ X_{PAO}$
K_{PHA}	Saturation coefficient for PHA	[1]	0.01	$g\ X_{PHA}\ g^{-1}\ X_{PAO}$

3.3. Model simulation of the biomass

The particulate component concentrations could be also calculated from model simulation as shown in Fig. 8 whereas the heterotrophic organism X_H; phosphate accumulating organism X_{PAO}, and autotrophic microorganism X_A concentrations in multi-tank AA/O activated sludge process were 638–1,204, 58.4–275, and 90–200.12 mg/L at run 1; 594.9–1321.4, 58.43–337.76, and 35–203.88 mg/L at run 2; 514.22–1,160, 58.42–271.13, and 95.5–208.6 mg/L at run 3; 534.26–1174.5, 58.42–272.5, and 89.72–185.36 mg/L at run 4. As result, The X_H; X_{PAO}; and X_A decreased in the anaerobic tank because of the lysis reaction. Then the heterotrophic organism X_H; phosphate accumulating organism $X_{PAO;}$ and autotrophic microorganism X_A increased in the aerobic tanks due to aerobic growth. The heterotrophic organism X_H; phosphate accumulating organism $X_{PAO;}$ and autotrophic microorganism X_A increased in quantities by about 56, 36, and 74% in tank one due to change the environmental state condition from anaerobic to aerobic and decreased in quantities by about 20, 44, and 0.14% in tank three due to change the environmental state condition from aerobic to anoxic. The ratio of total nitrifying species to total active biomass was between 1 and 12% in multi-tank AA/O process. In this study, the disadvantages of the developed BNR processes were improved by reconfiguring the process without mixed liquor and sludge recirculation. This was done by configuring the process into five-tank with variable environmental state conditions, anaerobic/anoxic, aerobic, and settling conditions, in each tank to achieve optimum removal of phosphorus and nitrogen. In multi-tank AA/O process, the intake location changing of raw wastewater was also used to direct the influent into the anoxic zone as an external carbon source for denitrification process. S_o, the heterotrophic organism X_H; phosphate accumulating organism X_{PAO}; and autotrophic microorganism X_A decreased in the anoxic tank due to the dilution effect of the flow. In addition to the dilution effect of the influent, the X_A also decreased due to the negative growth rate that resulted from lysis reaction in the anoxic tank. In full-scale wastewater treatment plant, the transient system behavior is of high practical importance since variations of composition, influent flow-rate as well as changes of operation prevent each real-world wastewater treatment plant from reaching the steady-state condition. Although the application of this ASM2d under steady state was validated in this study; the application in transient state can be implemented in the future study. In addition, the practical applications of the ASM2d model including plant optimization, controller layout, mathematical verification of the purification performance, and model-based state and parameter estimation should be taken into account in the future study.

4. Conclusions

The variation of pollutants COD, NH_4-N, NO_3-N, and PO_4-P in multi-tank AA/O activated sludge process could be modeled successfully using the activated sludge model No. 2d. The microbial kinetic behaviors in these testing four runs were analyzed based on ASM2d model. The results obtained in this study can be summarized as follows:

(1) The effective removal efficiency of COD, NH_4-N, TN, and TP at 89, 87.7, 73.6, and 83.7% were achieved, respectively, in multi-tank AA/O activated sludge process.
(2) In this study, the growth rate constant of autotrophic organisms X_A and its yield coefficient value were 1.4 day^{-1} and 0.14, respectively.
(3) According to model simulation, the X_H; X_{PAO}; and X_A concentrations 638–1,204, 58.4–275, and 90–200.12 mg/L at run 1, 594.9–1321.4, 58.43–337.76, and 35–203.88 mg/L at run 2, 514.22–1,160, 58.42–271.13, and 95.5–208.6 mg/L at run 3, 534.26–1174.5, 58.42–272.5, and 89.72–185.36 mg/L at run four in multi-tank AA/O activated sludge process.
(4) According to simulation, X_H; X_{PAO}; and X_A decreased in the anaerobic tanks because of the lysis reaction. Then the X_H; X_{PAO}; and X_A increased in the aerobic tanks due to aerobic growth. The X_H; X_{PAO}; and X_A increased in quantities by about 56, 36, and 74% in tank one due to change in the environmental state condition from anaerobic to aerobic and decreased in quantities

by about 20, 44, and 0.14% in the tank three due to change in the environmental state condition from aerobic to anoxic. The ratio of total nitrifying species to total active biomass was between 1 and 12% in multi-tank AA/O process.

Acknowledgments

This work was financially supported by the Major science and Technology program for water pollution control and treatment (No. 2012ZX07101-005) and Key Grant Project of National natural science foundation of China (Grant No. 51078074).

References

[1] M. Henze, W. Gujer, T. Mino, M.C.M. van Loosdrecht, Activated Sludge Models: ASM1, ASM2, ASM2d and ASM3, International Water Association, London, UK, 2000.
[2] WEF, Biological and Chemical Systems for Nutrient Removal, Water Environment Federation, Alexandria, Virginia, US, 1999.
[3] T.Y. Pai, Y.P. Tsai, Y.J. Chou, H.Y. Chang, H.G. Leu, C.F. Ouyang, Microbial kinetic analysis of three different types of EBNR process, Chemosphere 55(1) (2004) 109–118.
[4] T.Y. Pai, S.H. Chuang, Y.P. Tsai, C.F. Ouyang, Modelling a combined AAO and RBC process under DO variation by using an activated sludge—Biofilm hybrid model, J. Environ. Eng., ASCE 130(12) (2004) 1433–1441.
[5] T.Y. Pai, C.F. Ouyang, J.L. Su, H.K. Leu, Modeling the stable effluent qualities of the AAO process with Activated Sludge Model 2d under different return supernatant, J. Chin. Inst. Eng. 24(1) (2001) 75–84.
[6] T.Y. Pai, C.F. Ouyang, J.L. Su, H.K. Leu, Modelling the steady-state effluent characteristics of the TNCU process under different return mixed liquid, Appl. Math. Model. 25 (12) (2001) 1025–1038.
[7] J. Kappeler, R. Brodmann, Low F/M bulking and scumming: Towards a better understanding by modeling, Water Sci. Technol. 31(2) (1995) 225–234.
[8] S. Wyffels, S.W.H. Van Hulle, P. Boeckx, E.I.P. Volcke, O. Van Cleemput, P.A. Vanrolleghem, W. Verstraete, Modelling and simulation of oxygen-limited partial nitritation in a membrane-assisted bioreactor (MBR), Biotechnol. Bioeng. 86 (2004) 531–542.
[9] O. Nowak, K. Svardal, P. Schweighofer, The dynamic behaviour of nitrifying activated sludge systems influenced by inhibiting wastewater compounds, Water Sci. Technol. 31(2) (1995) 115–124.
[10] D. Wild, R. von Schulthess, W. Gujer, Structure modelling of denitrification intermediates, Water Sci. Technol. 31(2) (1995) 45–54.
[11] J. Copp, The COST Simulation Benchmark—Description and Simulator Manual, COST. European Cooperation in the Field of Scientific and Technical Research, Brussels, Belgium, 2001.
[12] J. Huo, R.B. Robinson, C.D. Cox, Uncertainty and sensitivity analysis of Activated Sludge Model No. 1 by Monte Carlo simulation for single CSTR with universal distribution parameters, in: Proceedings of the ASCE Conference, New York, 2004, p. 138.
[13] T. Mino, Activated sludge model: Microbiological basis, In: G. Bitton (Ed.), Encyclopedia of Environmental Microbiology, vol. 1, Wiley, New York, NY, pp. 14–26, 2002.
[14] D.R. Anderson, D.J. Sweeney, T.A. Williams, Statistics for Business and Economics (with Student CD-ROM, iPod Key Term, and InfoTrac), South-Western College Publishing, 2005.
[15] J. Wanner, J.S. Čech, M. Kos, New process design for biological nutrient removal, Water Sci. Technol. 25(4/5) (1992) 445–448.
[16] S.E.P.A. Chinese, Water and Wastewater Monitoring Methods, fourth ed., 2000, Chinese Environmental Science Publishing House, Beijing, China.
[17] APHA, AWWA, WEF, Standard Methods for the Examination of Water and Wastewater, 19th ed., American Public Health Association/American Water Works Association/Water Environment Federation, Washington, DC, 1995.
[18] H. Brouwer, M. Bloemen, B. Klapwijk, H. Spanjers, Feedforward control of nitrification by manipulating the aerobic volume in activated sludge plants, Water Sci. Technol. 38(3) (1998) 245–254.
[19] H. Brouwer, B. Klapwijk, M. Bloemen, Identification of activated sludge and wastewater characteristics using respirometric batch-experiments, Water. Res. 32(4) (1998) 1240–1254.
[20] U. Sollfrank, W. Gujer, Characterisation of domestic wastewater for mathematical modelling of activated sludge process, Water Sci. Technol. (Kyoto) 25 (1991) 1057–1066.
[21] G.H. Kristensen, P.E. Jorgensen, M. Henze, Characterization of functional microorganism groups and substrate in activated sludge and wastewater by AUR, NUR and OUR, Water Sci. Technol. 25(6) (1992) 43–57.
[22] T.Y. Pai, Y.P. Tsai, S.H. Chuang, W.C. Liao, Quantification of nitrifying species in the activated sludge process using OUR, NIRR and NARR, in: 2nd IWA Asian-Pacific Regional Conference, Bangkok, Thailand, 2003.
[23] T.Y. Pai, S.C. Wang, H.M. Lo, C.F. Chiang, M.H. Liu, R.J. Chiou et al., Novel modeling concept for evaluating the effects of cadmium and copper on heterotrophic growth and lysis rates in activated sludge process, J. Hazard. Mater. 166 (1) (2009) 200–206.
[24] G. Philippe, A. Jean-Mark, U. Vincent, B. Jean-Claude, Estimation of nitrifying bacterial activities by measuring oxygen uptake in the presence of the metabolic inhibitors allylthiourea and azide, Appl. Environ. Microbiol. 64 (1998) 2266–2268.
[25] G. Braunegg, B. Sonnleitner, R.M. Lafferty, A rapid gas chromatographic method for the determination of poly-b-hydroxybutyric acid in microbial biomass, J. Appl. Microbiol. Biotechnol. 6 (1978) 29–37.
[26] Henryk Melcer, Methods for Wastewater Characterization in Activated Sludge Modelling: Werf Report Project 99-wwf-3, IWA Publishing, 2003, ISBN: 1843396629, 9781843396628.
[27] C.F. Gerald, P.O. Wheatley, Applied Numerical Analysis, fourth ed., Addison-Wesley Publishing Company, 1989.